RMC a'la Kauland Thesis

http://mu2e-docdb.fnal.gov:8080/cgi-bin/ShowDocument?docid=521

Initialize

```
SetOptions[{Plot, ListPlot, LogPlot, LogLogPlot, ParametricPlot},
  Frame → True, AspectRatio → 1/GoldenRatio, PlotRange → All,
  th = 0.003; PlotRegion → Automatic, Axes → True, AxesLabel → True,
  AxesStyle → Automatic, GridLines → Automatic, PlotStyle →
   {{RGBColor[1, 0, 0], Thickness[th]}, {RGBColor[0, 1, 0], Thickness[th]},
    {RGBColor[0, 0, 1], Thickness[th]}, {RGBColor[0, 0, 0], Thickness[th]},
    {RGBColor[0, 0.8`, 0.8`], Thickness[th]}},
  BaseStyle → {FontSize → 10, FontWeight → "Bold"}];
```

3.3.3 The radiative muon capture process

$k^{\max,\mathrm{calc}} = m_\mu - \Delta M - m_e - R_{Z-1,A} - B_\mu$

with ΔM nuclear mass difference, $R_{Z-1,A}$ recoil energy, B_μ 1s binding energy.

Primakoff formula. Kaulard gives $(1 - 2x + 2x\text{^}2)(1-x)^2$. Based on e.g. ,Rood NP 70 (1965) 658, I believe the correct formula is $(1 - 2x + 2x\text{^}2)x(1-x)^2$.

```
Clear[k, kmax];
f[k_, kmax_] := (x = k / kmax; If[x < 1, 20 (1 - 2 x + 2 x^2) x (1 - x)^2, 0.])
```

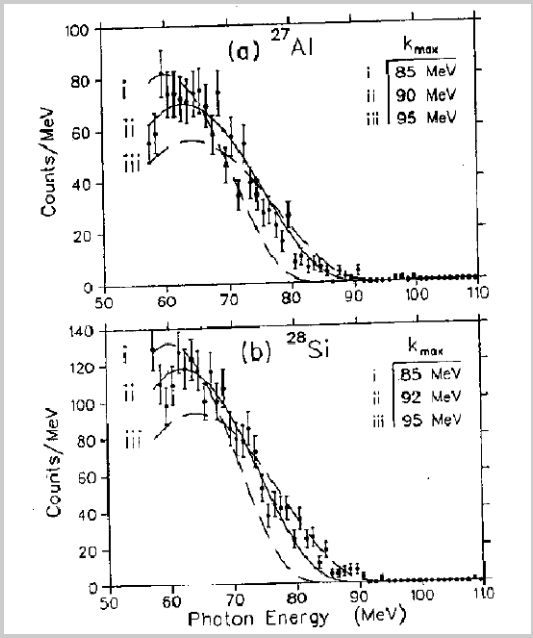

A	rel. Anteil in [%]	m_{Ti} in $[MeV/c^2]$	m_{Sc} in $[MeV/c^2]$	$E_\gamma^{max,calc}$ in $[MeV]$	$E_\gamma^{max,Ca}$ in $[MeV]$	$E_{\beta^-\epsilon^+}^{gs}$ in $[MeV]$
46	7.94	42804.95	42807.3	100.88	91.38 ± 2	102.26
47	7.44	43735.64	43736.2	102.65	93.15 ± 2	100.66
48	73.78	44663.56	44667.6	99.24	89.74 ± 2	98.99
49	5.51	45595.02	45597.0	101.25	91.75 ± 2	95.98
50	5.34	46523.65	46530.5	96.38	86.88 ± 2	91.39

Massen nach [10]
relative Anteile nach [51]

The Primakoff formula describes the shape of the measured RMC spectra, if kmax is taken as a fit parameter. For Ca one finds a kmax,Ca which is 9.5 MeV lower than kmax calculated. It is assumed that shift corresponds to some average nuclear excitation. In the table above the same shift is also assumed for the other elements. The Primakoff Model overestimates the RMC rate.

The experimental fraction of RMC/OMC for k>57 MeV is estimated to be 2.0±0.5 10^{-5}.

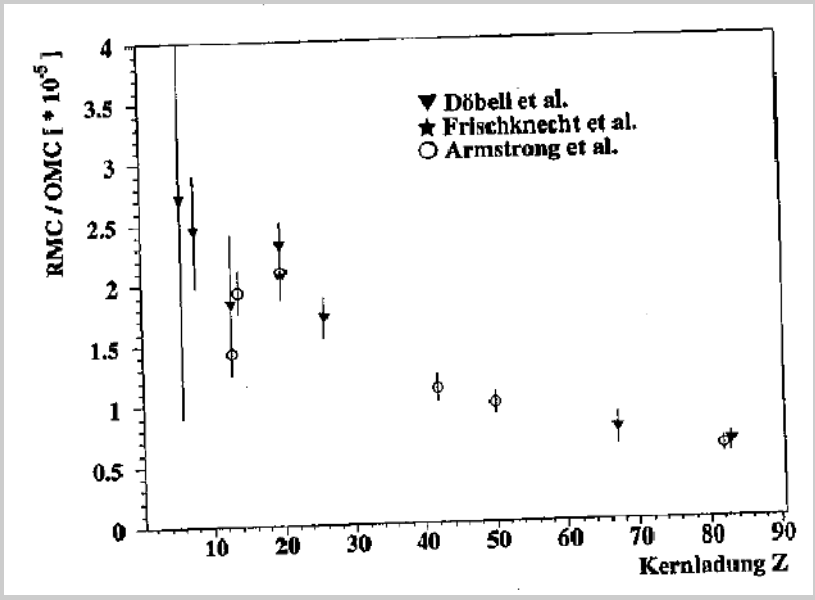

5.4 Simulation of RMC

```
kmc = 99.2; kmca = 89.7 ;(* A=48 *)
fscal = 2 × 10^-5;
fsc = fscal / Integrate[f[k, kmc], {k, 57, kmc}];
fsca = fscal / Integrate[f[k, kmca], {k, 57, kmca}];
Plot[{f[k, kmca] fsca, f[k, kmc] fsc},
 {k, 70, kmca}, FrameLabel → {"k (MeV)", "P (MeV)"}]
ScientificForm[{Integrate[f[k, kmca] fsca, {k, 80, kmca}] ,
  Integrate[f[k, kmca] fsca, {k, 57, kmca}]}]
```

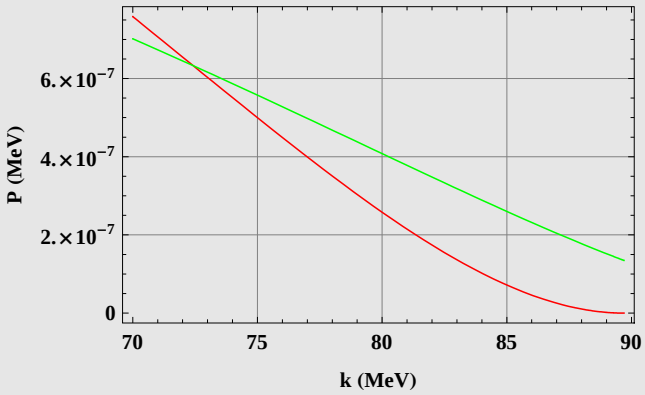

$\{9.08372\times10^{-7},\ 2.\times10^{-5}\}$

Kauland gives $P\gamma$(k>80 MeV)= 1.02 10^{-6} per OMC. I get 0.9 10^{-6}. For positrons this MC gives Pe(k>80 MeV) =2.6 10^{-11} per OMC, for the SINDRUM setup.

```
PosPerRMC = 2.6 × 10^-11 / 10^-6; ScientificForm[PosPerRMC]
```

2.6×10^{-5}

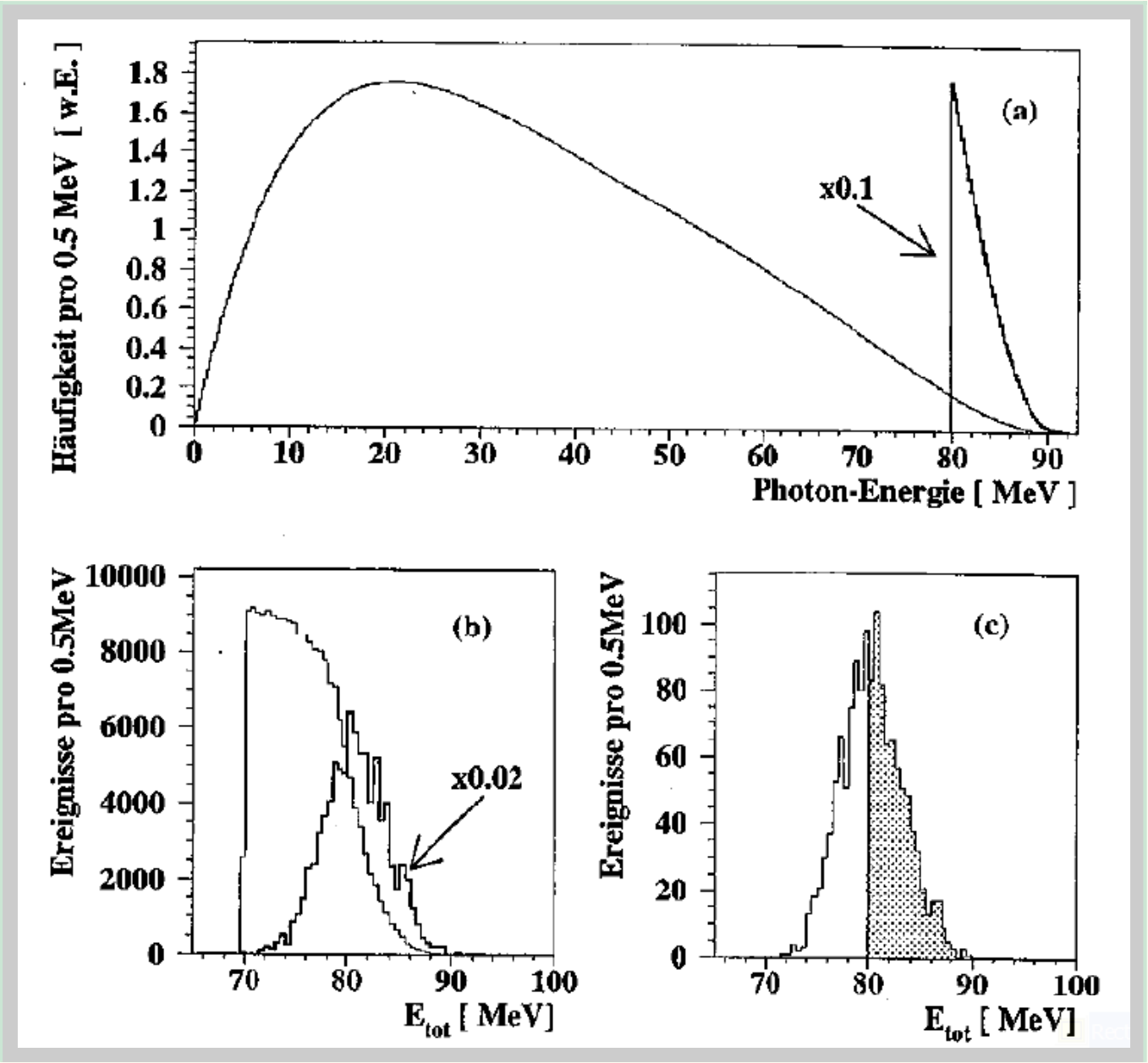

7.3 Discussion RMC continuum

Kauland finds more high energy positrons than explained by the Primakoff formula. If one assumes a 3% contribution of ~93 MeV gammas, the positron spectrum can be fitted.

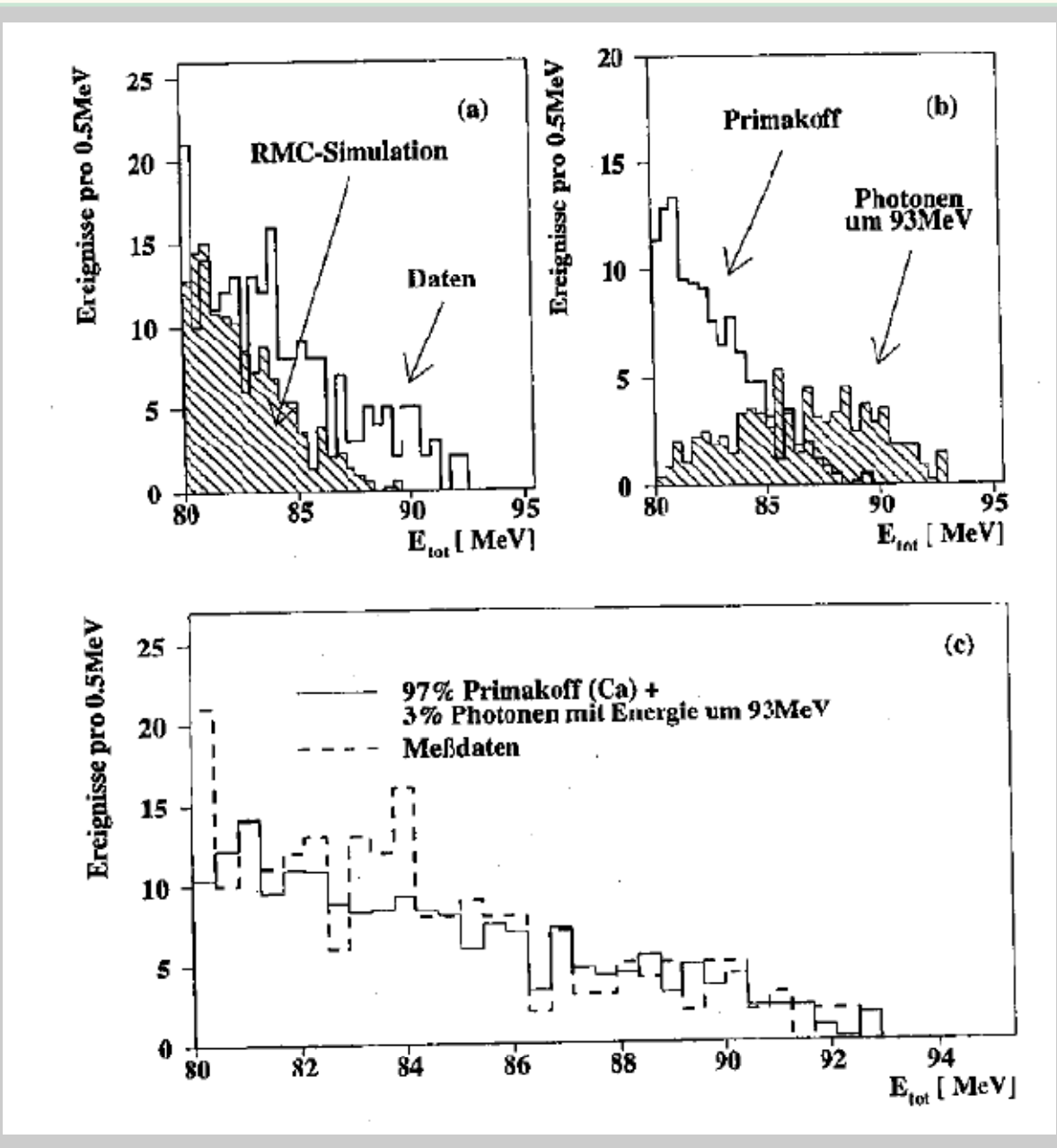
(a)
RMC-Simulation
Daten
Ereignisse pro 0.5MeV
E_{tot} [MeV]
(b)
Primakoff
Photonen
um 93MeV
Ereignisse pro 0.5MeV
E_{tot} [MeV]
(c)
97% Primakoff (Ca) +
3% Photonen mit Energie um 93MeV
Meßdaten
Ereignisse pro 0.5MeV
E_{tot} [MeV]

Radiative muon capture on O, Al, Si, Ti, Zr, and Ag
Bergbusch, P.C. et al., Physical Review C 59, 2853-64, 1999

D. RMC in Ti as a background to μ-e conversion

RMC is a major background for μ-e conversion experiments, many of which use Ti as a target [39]. This background arises from the asymmetric conversion of RMC photons in which a high energy positron is produced. Before now, RMC on Ti had never been measured so the experimental branching ratio for Ca was used, corrected by a factor of 0.91 to account for the Z dependence of the RMC to OMC ratio. To fit the PSI data [39], a Primakoff polynomial spectral shape was assumed and applied to each Ti isotope. The end point photon energy for each isotope was determined by subtracting from the kinematical RMC end point the same amount subtracted in the Ca case. This was found to be insufficient to describe the observed background; so an additional spectrum with a 93 MeV end point was added.

The present measurement of the RMC rate in Ti ($R_\gamma = 1.30\times10^{-5}$) is significantly lower than the 1.93×10^{-5} assumed in Ref. [39]. Also, the best fit of the end point energy k_{max} to the spectrum is 89.2 MeV, a bit lower than the assumed value of 89.7 MeV for the dominant Ti isotope. As shown in Fig. 14, there appears to be no evidence of RMC photons between 89 and 93 MeV, which implies that the observed background in μ-e conversion does not result from the RMC process.

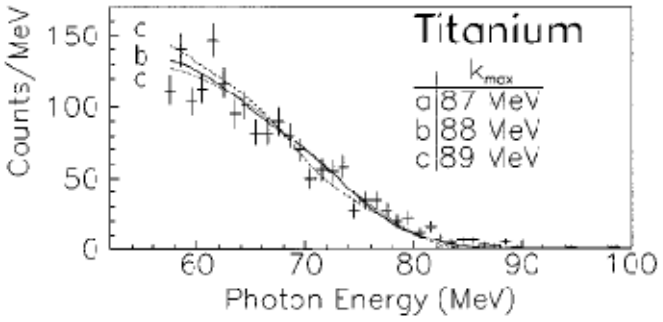

FIG. 14. Comparison of the experimental RMC on Ti photon spectrum (error bars) with the closure spectral shape of Eq. (7) after convolution with the spectrometer response and software cuts. The solid line is the spectral shape for the best fit value of k_{max}.

Gorringe & Fearing review

TABLE XIV. Summary of the world data on the quantity R_γ on $A>3$ targets, where R_γ is the ratio of the radiative muon capture rate with $E_\gamma>57$ MeV to the ordinary muon capture rate in units of 10^{-5}. In order to assist comparisons in most cases the quoted results are for the closure approximation spectra shape where the corresponding value of the parameter k_{max} is given in column 4. The quantity α is the neutron excess $(A-2Z)/Z$.

Target	α	R_γ ($\times 10^{-5}$)	k_{max} (MeV)
Bergbusch *et al.* (1999)			
$^{16}_{8}$O	0.000	1.67±0.18	88.4±2.3
$^{27}_{13}$Al	0.077	1.43±0.11	90.1±1.8
$^{28}_{14}$Si	0.000	2.09±0.20	89.4±1.8
$^{nat}_{22}$Ti	0.173	1.30±0.12	89.2±2.0
$^{nat}_{40}$Zr	0.280	1.31±0.15	89.2±3.4
$^{nat}_{47}$Ag	0.296	1.12±0.13	89.0±3.2
Gorringe *et al.* (1998)			
$^{58}_{28}$Ni	0.071	1.48±0.08	92.0±2.0
$^{60}_{28}$Ni	0.143	1.39±0.09	90.0±2.0
$^{62}_{28}$Ni	0.214	1.05±0.06	89.0±2.0
Armstrong *et al.* (1992)			
$^{27}_{13}$Al	0.077	1.43±0.13	90.0±2.0
$^{28}_{14}$Si	0.000	1.93±0.18	92.0±2.0
$^{40}_{20}$Ca	0.000	2.09±0.19	93.0±2.0
$^{nat}_{42}$Mo	0.283	1.11±0.11	90.0±2.0
$^{nat}_{50}$Sn	0.374	0.98±0.09	87.0±2.0
$^{nat}_{82}$Pb	0.527	0.60±0.07	84.0±3.0
Armstrong *et al.* (1991)			
$^{12}_{6}$C	0.000	1.98±0.20	
$^{16}_{8}$O	0.000	2.18±0.20	
$^{40}_{20}$Ca	0.000	2.04±0.14	
Frischknecht *et al.* (1988)			
$^{16}_{8}$O	0.000	3.80±0.40	
Döbeli *et al.* (1986)			
$^{12}_{6}$C	0.000	2.70±1.80	
$^{16}_{8}$O	0.000	2.44±0.47	89.9±5.0
$^{27}_{13}$Al	0.077	1.83±0.26	88.8±1.8
$^{40}_{20}$Ca	0.000	2.30±0.21	92.5±0.7
$^{nat}_{26}$Fe	0.146	1.71±0.17	90.2±1.1
$^{165}_{67}$Ho	0.463	0.75±0.13	84.1±5.1
$^{209}_{83}$Bi	0.518	0.62±0.08	88.2±0.6
Frischknecht *et al.* (1985)			
$^{40}_{20}$Ca	0.000	1.92±0.20	90.8±0.9
Hart *et al.* (1977)			
$^{40}_{20}$Ca	0.000	2.11±0.14	86.5±1.9